

Eigenstate Gibbs Ensemble in Integrable Quantum Systems

Sourav Nandy¹, Arnab Sen¹, Arnab Das¹, Abhishek Dhar²

¹*Department of Theoretical Physics, Indian Association for the Cultivation of Science, Jadavpur, Kolkata 700032, India.*

²*International Centre for Theoretical Sciences, TIFR, Shivakote Village, Hesaraghatta Hobli, Bengaluru 560089, India.*

(Dated: January 20, 2021)

The Eigenstate Thermalization Hypothesis implies that for a thermodynamically large system in one of its eigenstates, the reduced density matrix describing any finite subsystem is determined solely by a set of *relevant* conserved quantities. In a generic system, only the energy plays that role and hence eigenstates appear locally thermal. Integrable systems, on the other hand, possess an extensive number of such conserved quantities and hence the reduced density matrix requires specification of an infinite number of parameters (Generalized Gibbs Ensemble). However, here we show by unbiased statistical sampling of the individual eigenstates with a given finite energy density, that the local description of an overwhelming majority of these states of even such an integrable system is actually Gibbs-like, i.e. requires only the energy density of the eigenstate. Rare eigenstates that cannot be represented by the Gibbs ensemble can also be sampled efficiently by our method and their local properties are then shown to be described by appropriately *truncated* Generalized Gibbs Ensembles. We further show that the presence of these rare eigenstates differentiates the model from the generic (non-integrable) case and leads to the system being described by a Generalized Gibbs Ensemble at long time under a unitary dynamics following a sudden quench, even when the initial state is a Gibbs-like eigenstate of the pre-quench Hamiltonian.

I. INTRODUCTION

The question of thermalization, i.e., whether or not a closed many-body quantum system can act as a heat-bath for its own subsystems when the rest of the system is much bigger, has remained an open issue of fundamental importance since the inception of quantum mechanics. The basis for classical statistical mechanics is the hypothesis of equal a priori probability (EAP), which states that all microstates with equal energy are equally likely to occur during the time evolution of a closed generic (interacting) system (see, e.g., [1]). This gives a possible justification of the use of the microcanonical ensemble. On the other hand, a quantum many-body system, prepared in an energy eigenstate, remains in the same energy state. In this case, EAP is extended to the level of single many-body eigenstates resulting in the Eigenstate Thermalization Hypothesis (ETH) [2–5]. ETH implies that even if a generic many-body system is kept in one of its eigenstates, its (local) subsystems are provided with enough quantum fluctuations by the rest of the system, so that they can be described by the most general (unbiased) ensemble compatible with the conservation of energy of the total system. Thus suppose that the total system, described by a Hamiltonian H , is in an eigenstate $|\psi\rangle$, and is described by the corresponding density matrix $\rho = |\psi\rangle\langle\psi|$. Then it is expected that the reduced density matrix of the subsystem \mathcal{S} , $\rho_{\mathcal{S}} = \text{Tr}_{\bar{\mathcal{S}}}\rho$, obtained by integrating out its complement $\bar{\mathcal{S}}$, should be described by an effective density matrix of the form $\text{Tr}_{\bar{\mathcal{S}}}\rho_{\text{GGE}}$, where $\rho_{\text{GGE}} = \frac{1}{\mathcal{Z}} \exp^{-\beta H}$, with \mathcal{Z} being the relevant normalization constant (partition function), and the parameter β (inverse temperature) is fixed solely by requiring that ρ_{GGE} gives an energy density which equals that of the eigenstate. ETH was implicit in the founda-

tions of quantum statistical mechanics (see, e.g., [1, 6]).

However, there are important classes of systems e.g., those which can be mapped to non-interacting degrees of freedom (see, e.g., [7, 8]), where there are infinitely many (of the order of the size of the system) *relevant* conserved quantities that restricts the statistical distributions of the subsystems. If one used an entropy maximisation principle (as in [9]), these conserved quantities are to be treated in the same footing as energy, and that implies a “generalized” Gibbs ensemble (GGE) for the subsystem, which is characterized by as many parameters as there are conserved quantities [9]. Extension of this to the eigenstate level implies a restricted (generalized) ETH: such systems would effectively be described by a reduced density matrix of the form $\text{Tr}_{\bar{\mathcal{S}}}\rho_{\text{GGE}}$, where $\rho_{\text{GGE}} = \exp\left[-\sum_i^{\mathcal{N}_L} \lambda_i \hat{\mathcal{I}}_i\right] / \mathcal{Z}$, where $\hat{\mathcal{I}}_i$ denotes the relevant integrals of motion, λ_i are their corresponding Lagrange multipliers and \mathcal{N}_L is proportional to the system size [9–12]. An important question here is whether *all* the integrals of motion $\hat{\mathcal{I}}_i$ are necessary to describe the properties of a finite subsystem. This idea of equilibrium statistical mechanics has been extended to describe the asymptotic synchronized states of periodically driven non-interacting systems (or those mappable to it) using periodic Gibbs’ ensemble [13], hence the question is not necessarily limited to the domain of equilibrium statistical mechanics.

Another related approach to thermalization is to start from a pure state, usually the ground state of a local (pre-quench) Hamiltonian, that is not an eigenstate of the system’s final (post-quench) Hamiltonian, and let it evolve in time under the resulting unitary dynamics [4, 10, 14–16]. If the system can act as its own reservoir, as ETH implies, then the long-time evolved state can also be described by a thermal density matrix as far as local opera-

tors are concerned. However, if the evolution of the state is due to an integrable Hamiltonian, the long time behavior of local operators should instead be again described by a GGE (and not GE) which respects the extensive number of conservation laws forced by the unitary dynamics of the (post-quench) Hamiltonian. Whether the infinite amount of information regarding all the conserved quantities $\hat{\mathcal{L}}_i$ is really necessary to understand local properties is again an important issue in describing steady states that eventually arise from such dynamics.

In this work, we consider the finite energy density eigenstates of the transverse field Ising model (TFIM) in one dimension (1D) and study the reduced density matrices (RDMs) and local correlation functions in subsystems of l consecutive spins by performing an unbiased sampling of the individual eigenstates in chains of linear dimension L (with L ranging upto 10^5 spins). By doing a careful finite-size scaling, we find that the RDMs of a *typical* finite energy density eigenstate approaches the standard GE form (and not a GGE) determined only by the energy density of the eigenstate for $l \ll L$, but not for finite l/L , as $L \rightarrow \infty$. This is inspite of the integrable nature of the model and is because the densities of all the additional “local” conserved quantities approach their “thermal” values as $L \rightarrow \infty$, and so the corresponding Lagrange multipliers vanish. This provides an explicit example of *weak* ETH [17, 18] where typical (but not all) energy eigenstates appear thermal when local correlation functions are probed. We note that such a weak ETH scenario has been recently numerically demonstrated in a different kind of (Bethe integrable) spin model [19] and a Bose gas [20] in one dimension. However, only the infinite temperature ensemble was considered in Ref. 19, while we have no such restriction on the average energy density of the sampled eigenstates. Moreover these studies obtained eigenstates using Bethe ansatz, and so were limited to small system sizes. Furthermore, we also consider the local properties of the rare eigenstates where the effects of the other integrals of motion (apart from the Hamiltonian) becomes apparent. The presence of (rare) eigenstates which do not follow a GE locally in the thermodynamic limit is a consequence of the integrability of the model, since such states are believed to be absent in a generic system (for numerical tests of the same, see Refs. 21–23). The fraction of such rare eigenstates shrinks to zero in the thermodynamic limit but these can also be sampled efficiently by our method and their local properties are then shown to be described by RDMs that approach appropriate “truncated” GGEs as $L \rightarrow \infty$ and $l \ll L$ where only a *few* ($\mathcal{O}(1)$) integrals of motion need to be retained for an accurate description for a majority of such states.

Furthermore, we also consider a sudden quench of the magnetic field in the 1D TFIM where the initial state is not the ground state of the pre-quench Hamiltonian (see also Ref. 24) but instead a typical finite energy density eigenstate, and study the nature of the steady state obtained at asymptotically large times. We show that even

though the initial (pure) state is locally thermal, the final state needs a full GGE description for its local properties. The behaviour of the Lagrange multipliers in the GGE however has important differences compared to a quench starting from the ground state of the pre-quench Hamiltonian [25], which we point out here.

The rest of the paper is arranged in the following manner. In Sec. II, we review some results relevant for our work and set the notations for the rest of the paper. In Sec. III, we describe our numerical procedure for sampling any given finite energy density eigenstates of the 1D TFIM in chains of size L . The behaviour of the typical eigenstates is described in Sec. IV, and we consider the rare eigenstates that requires a GGE description in Sec. V. In Sec. VI, we obtain an analytic expression for the GGE which describes the steady state after a quench, where the initial state is a typical finite energy density eigenstate. Finally, we summarize our results and conclude in Sec. VII.

II. 1D TFIM: SOME PRELIMINARIES

The 1D TFIM is defined by the following Hamiltonian:

$$H = - \sum_{j=1}^L (g\sigma_j^x + \sigma_j^z \sigma_{j+1}^z) \quad (1)$$

where $\sigma^{x,y,z}$ are the Pauli operators and the external magnetic field equals g . We further impose periodic boundary condition ($\sigma_{L+1}^\alpha = \sigma_1^\alpha$ where $\alpha = x, y, z$) with L being even. The ground state of this model is ferromagnetic when $-1 < g < 1$ and paramagnetic otherwise, with continuous quantum critical points at $g = \pm 1$ [8].

This model can be solved exactly for any finite L using a well-known mapping of the spins to *spinless fermions* (Jordan-Wigner transformation) (e.g. see Ref. 7 and 8):

$$\begin{aligned} \sigma_n^x &= 1 - 2c_n^\dagger c_n \\ \sigma_n^z &= -(c_n + c_n^\dagger) \prod_{m=1}^{n-1} (1 - 2c_m^\dagger c_m) \end{aligned} \quad (2)$$

From Eq. 2, the vacuum state of the c fermions, which we denote by $|0\rangle$, corresponds to $\sigma^x = +1$ for all sites. Writing H (Eqn. 1) in terms of these fermions, we obtain (after omitting constant terms)

$$\begin{aligned} H &= 2g \sum_{j=1}^L c_j^\dagger c_j - \sum_{j=1}^{L-1} \left(c_j^\dagger c_{j+1} + c_j^\dagger c_{j+1}^\dagger + \text{h.c.} \right) \\ &+ (-1)^{N_F} [c_L^\dagger c_1 + c_L^\dagger c_1^\dagger + \text{h.c.}] \end{aligned} \quad (3)$$

The sign of the boundary term depends on whether the total number N_F of the c fermions is odd or even. If N_F is odd, periodic boundary conditions on the fermions is required ($c_{L+1} = c_1$), whereas for N_F even, antiperiodic boundary condition is imposed ($c_{L+1} = -c_1$). Since the Hamiltonian conserves fermion parity, these sectors do

not mix and we restrict ourselves to even N_F for the rest of this paper.

To diagonalize the Hamiltonian, we go to momentum space and accordingly define

$$c_k = \frac{\exp(i\pi/4)}{\sqrt{L}} \sum_x \exp(-ikx) c_x \quad (4)$$

where $k = 2\pi m/L$ with $m = -(L-1)/2, \dots, -1/2, 1/2, \dots, (L-1)/2$. Re-writing H in terms of c_k, c_k^\dagger , we get $H = \sum_{k>0} H_k$ where

$$H_k = 2(g - \cos(k)) [c_k^\dagger c_k - c_{-k} c_{-k}^\dagger] + 2 \sin(k) [c_{-k} c_k + c_k^\dagger c_{-k}^\dagger]. \quad (5)$$

This Hamiltonian connects the vacuum (of the c fermions) $|0\rangle$ with $|k, -k\rangle = c_k^\dagger c_{-k}^\dagger |0\rangle$, and $|k\rangle = c_k^\dagger |0\rangle$ with $|-k\rangle = c_{-k}^\dagger |0\rangle$.

We further restrict ourselves to the parity invariant states (PIS) in which all the positive and negative momentum modes are populated with the same weights. All the eigenstates $|\psi\rangle$ of the TFIM at a magnetic field strength g which are also PIS can then be written in the form

$$|\psi\rangle = \otimes_{k>0} |\psi_k\rangle \\ |\psi_k\rangle = U_{kn}(g) c_k^\dagger c_{-k}^\dagger |0\rangle + V_{kn}(g) |0\rangle \quad (6)$$

where $(U_{kn}(g), V_{kn}(g))$ can only have either of the two forms shown below at each k to be an eigenstate:

$$(U_{k0}(g), V_{k0}(g)) = \left(-\sin\left(\frac{\theta_k^g}{2}\right), \cos\left(\frac{\theta_k^g}{2}\right) \right) \\ (U_{k1}(g), V_{k1}(g)) = \left(-\cos\left(\frac{\theta_k^g}{2}\right), -\sin\left(\frac{\theta_k^g}{2}\right) \right) \\ \sin(\theta_k^g) = \frac{\sin(k)}{\sqrt{(g - \cos(k))^2 + (\sin(k))^2}} \quad (7)$$

These eigenstates can be equivalently represented by strings with either 0 or 1 at each $k > 0$, which we denote by the label n_k , where 0(1) refers to $(U_{k0(1)}(g), V_{k0(1)}(g))$. The total energy of such an eigenstate is given by

$$E = \sum_{k>0} \epsilon_k(g) (2n_k - 1) \\ \epsilon_k(g) = 2\sqrt{(g - \cos(k))^2 + (\sin(k))^2} \quad (8)$$

These states represent $2^{L/2}$ of the 2^L eigenstates of the TFIM (including its ground state) in a chain of length L and we will focus exclusively on these states in this study. A quantum quench (by suddenly changing the magnetic field g) in which the initial state is such an eigenstate of the TFIM continues to be a PIS (though not an eigenstate of the post-quench Hamiltonian) under the unitary dynamics.

For completeness, note that H_k in Eq. 5 can be easily diagonalized through a Bogoliubov rotation with an angle $\theta_k^g/2$ (with θ_k^g as defined in Eq. 7) to give

$$H = \sum_{k>0} \epsilon_k(g) (\mathcal{A}_k^\dagger \mathcal{A}_k + \mathcal{A}_{-k}^\dagger \mathcal{A}_{-k} - 1) \quad (9)$$

with $\mathcal{A}_k = V_{k0}^*(g) c_k - U_{-k0}(g) c_{-k}^\dagger$ denoting the Bogoliubov fermion operator at momentum k . Thus n_k equals $\mathcal{A}_k^\dagger \mathcal{A}_k = 0(1)$ and represents such an unoccupied (occupied) single-particle level at momentum k . Since we are considering parity invariant eigenstates, the Bogoliubov fermions at k and $-k$ are always (un)occupied in pairs giving Eq. 8 from Eq. 9.

A. Local properties of individual eigenstates

1. Generalized Gibbs ensemble

To write down the GGE description for the individual eigenstates (Eq. 6) in the TFIM or for the steady state obtained after a quantum quench, we need to specify the extensive number of integrals of motion \hat{I}_i present in the model. From the (non-local) mapping of the spins to free fermions using the Jordan-Wigner transformation as discussed in the previous section, it is clear that the average occupation number of the Bogoliubov fermion at each momentum k , i.e. $n_k = \mathcal{A}_k^\dagger \mathcal{A}_k$, is a conserved quantity and the number of such conserved quantities scales extensively with L . For the case of quantum quenches, the following GGE construction [10, 11] has been shown to provide the correct description for properties of the steady state of the system:

$$\rho_{\text{GGE}} = \frac{1}{\mathcal{Z}} \exp\left(-\sum_k \lambda_k n_k\right) \quad (10)$$

where the Lagrange multiplier λ_k is defined as

$$\lambda_k = \log\left(\frac{1 - \langle n_k \rangle}{\langle n_k \rangle}\right) \quad (11)$$

with $\langle n_k \rangle = \langle \psi | \mathcal{A}_k^\dagger \mathcal{A}_k | \psi \rangle$, where $\mathcal{A}_k^\dagger \mathcal{A}_k$ refers to the Bogoliubov fermion occupation of the post-quench Hamiltonian in case of the quantum quench.

This form of the GGE, however, does not make it clear as to which conserved quantities need to be retained and which can be ignored when describing local properties of the system, since the occupation numbers n_k are *non-local* in real space. Moreover, these conservations do not possess corresponding local densities, unlike the Hamiltonian. Another problem with this form of ρ_{GGE} arises when considering exact eigenstates of the TFIM, and not the steady state following a quench, since there the corresponding Lagrange multipliers λ_k are not defined microscopically as each n_k can only be 0 or 1.

An equivalent representation of ρ_{GGE} was recently constructed by Fagotti and Essler for the TFIM [25] where only the local (in space) conservations I_n^\pm (where n is a non-negative integer) present in the model were considered for constructing the GGE. Each such I_n^\pm involves $n+2$ neighboring spins but can be written in a straightforward manner in terms of the occupations numbers

n_k [25] as

$$\begin{aligned} I_n^+ &= \sum_k \cos(nk) \epsilon_k(g) n_k \\ I_n^- &= - \sum_k 2 \sin[(n+1)k] n_k \end{aligned} \quad (12)$$

Again, it is implicit here that n_k in the definition of I_n^\pm refers to the average Bogoliubov fermion occupation of the post-quench Hamiltonian in the case of a quantum quench.

The GGE can now be defined in terms of these local integrals of motion as

$$\rho_{\text{GGE}} = \frac{1}{\mathcal{Z}} \exp \left(- \sum_{n=0}^{(L/2)-1} \sum_{\sigma=\pm} [\lambda_n^\sigma I_n^\sigma] \right) \quad (13)$$

where the Lagrange multipliers λ_n^σ are fixed by the conditions:

$$\text{Tr}[\rho_{\text{GGE}} I_n^\sigma] = \langle \psi | I_n^\sigma | \psi \rangle. \quad (14)$$

This representation of the RDMs serves as the ideal starting point for the issues that we address here. Firstly, as was shown in Ref. 25 for the case of quantum quenches in the TFIM, the properties of local subsystems with l consecutive spins in the final steady state can be understood by only considering the y most local conservation laws, i.e.,

$$\rho_{\text{GGE}}^{(y)} = \frac{1}{\mathcal{Z}_y} \exp \left(- \sum_{n=0}^{y-1} \sum_{\sigma=\pm} [\lambda_{n,y}^\sigma I_n^\sigma] \right) \quad (15)$$

where $y \sim \mathcal{O}(l)$ gives a very good description of the subsystem properties and including more non-local conservation laws only gives an exponentially small $\exp(-y)$ correction thereafter. Thus, for describing the properties of subsystems of size l , I_n^σ with $n \gg l$ can be completely ignored. We will show later that similar behaviour occurs for the RDMs for l consecutive spins when finite energy density eigenstates of the TFIM are considered, with $y \sim \mathcal{O}(l)$ providing a very good description of the subsystem. Secondly, unlike λ_k , the Lagrange multipliers $\lambda_{n,y}^\sigma$ are well-defined microscopically for the eigenstates.

For the eigenstates which are also PIS (Eqn. 6), it is easy to see that $I_n^- = 0$ because $n_k = n_{-k}$ (Eqn. 12). Thus, we need to only consider the integrals of motion I_n^+ and will henceforth suppress the index $+$ from both I_n^+ and λ_n^+ . Also, I_0 equals the total energy of the system (shifted such that the ground state has zero energy) and thus the Lagrange multiplier λ_0 can be identified with the inverse temperature β . Since both the descriptions of ρ_{GGE} are equivalent (Eqn. 10 and Eqn. 13), it is possible to transform from λ_k to λ_n by using:

$$\lambda_n = \left(\frac{2 - \delta_{n,0}}{L} \right) \sum_{k>0} \frac{\lambda_k}{\epsilon_k} \cos(nk). \quad (16)$$

2. Reduced density matrices and the distance measure

We proceed in a similar way to Ref. 26 to calculate the entanglement of l adjacent spins for the TFIM. The RDMs for any individual eigenstate of the form Eqn. 6 is most simply calculated after expressing that state in terms of the c fermions. Since the transformation between the spins and the fermions is non-local, we *cannot* express the RDM of l non-adjacent spins in any simple manner in terms of the fermion correlations involving only the sites within the subsystem. However, if we take l adjacent spins as the subsystem, then all the non-zero spin correlations involving any subset of these l sites for a finite L can be expressed in terms of the fermionic correlation functions at these l sites [27, 28]. This is straightforward to see for correlation functions involving σ_n^x only since these are local in terms of the c fermions. Moreover, even for correlations functions involving an even number of σ_n^z , (σ_n^z being non-local in terms of the c fermions, see Eqn. 2), the Jorgan-Wigner strings outside the subsystem cancel and the resulting expression is in terms of the fermions within the subsystem only. Correlations functions with an odd number of σ_n^z are zero due to the \mathcal{Z}_2 symmetry of the model. The RDM can then be calculated solely by considering the correlation functions of the fermions in the subsystem. Furthermore, since the fermions are non-interacting, all higher point fermionic correlators can be calculated from the two-point correlation functions using Wick's theorem [29].

The two-point fermionic correlations can be expressed in terms of two $l \times l$ matrices [29], \mathbf{C} and \mathbf{F} , whose elements are constructed by knowing $(U_{kn}(g), V_{kn}(g))$ for the eigenstate $|\psi\rangle$ (Eqn. 6 and Eqn. 7):

$$\begin{aligned} C_{ij} &= \langle \psi | c_i^\dagger c_j | \psi \rangle = \frac{2}{L} \sum_{k>0} |U_{kn}(g)|^2 \cos(k(i-j)) \\ F_{ij} &= \langle \psi | c_i^\dagger c_j^\dagger | \psi \rangle = \frac{2}{L} \sum_{k>0} U_{kn}^*(g) V_{kn}(g) \sin(k(i-j)) \end{aligned} \quad (17)$$

where i, j refer to sites in the subsystem.

The RDM for a block of l adjacent spins may then be written in terms of the c fermions as

$$\begin{aligned} \rho_S &= \frac{1}{\mathcal{Z}_S} \exp(-\mathcal{H}_S), \\ \mathcal{H}_S &= \sum_{k=1}^l \mathcal{E}_{k,S} \eta_{k,S}^\dagger \eta_{k,S} \end{aligned} \quad (18)$$

where \mathcal{H}_S denotes its ‘‘entanglement Hamiltonian’’ which is diagonal in terms of operators $\eta_{k,S}, \eta_{k,S}^\dagger$ that are fermionic operators for single particle states with energies $\mathcal{E}_{k,S}$ and linearly related to the operators c_i, c_i^\dagger . \mathcal{Z}_S ensures the correct normalization $\text{Tr}(\rho_S) = 1$.

Since *all* correlation functions of the subsystem can be expressed in terms of the quadratic fermionic correlations by using Wick's Theorem here, the entanglement

Hamiltonian \mathcal{H}_S , and hence ρ_S , is fully determined by the condition that it gives the *right* quadratic correlation functions C_{ij} and F_{ij} for the sites that belong to the subsystem [29]. Calculating ρ_S thus requires only the eigenvectors and eigenvalues of the $2l \times 2l$ matrix \mathcal{C} defined as

$$\begin{pmatrix} \mathbf{I} - \mathbf{C} & \mathbf{F}^\dagger \\ \mathbf{F} & \mathbf{C} \end{pmatrix} \quad (19)$$

Particularly, the entanglement entropy of the subsystem $S_{ent}(l)$ only requires the eigenvalues:

$$\begin{aligned} S_{ent}(l) &= -\text{Tr}(\rho_S \log \rho_S) \\ &= -\sum_{k=1}^{2l} p_k \log(p_k) \end{aligned} \quad (20)$$

where p_k denotes the eigenvalue of the \mathcal{C} matrix.

We now define a distance measure for the RDMs in an eigenstate $|\psi\rangle$ to quantify how well these operators are described by the truncated GGEs based on a few local integrals of motion. Since all the local conservations I_n are quadratic in the c fermions (Eqn. 12), one can simply define the distance measure using the correlation matrices $\mathcal{C}(l)$ and $\mathcal{C}_{\text{GGE}}^{(y)}(l)$ [30], where the latter is calculated assuming the density matrix of the full system to be $\rho_{\text{GGE}}^{(y)}$ (Eqn. 15). We use the standard trace distance between these two matrices to define the distance measure $\mathcal{D}(\mathcal{C}(l), \mathcal{C}_{\text{GGE}}^{(y)}(l))$ as

$$\frac{1}{2l} \text{Tr} \sqrt{(\mathcal{C}_{\text{GGE}}^{(y)}(l) - \mathcal{C}(l))^\dagger (\mathcal{C}_{\text{GGE}}^{(y)}(l) - \mathcal{C}(l))} \quad (21)$$

Note that $0 \leq \mathcal{D}(\mathcal{C}(l), \mathcal{C}_{\text{GGE}}^{(y)}(l)) \leq 1$ and is identically zero only when $\mathcal{C}_{\text{GGE}}^{(y)}(l) = \mathcal{C}(l)$. When $\mathcal{D}(\mathcal{C}(l), \mathcal{C}_{\text{GGE}}^{(y)}(l)) = 0$, it implies that all the (non-zero) correlation functions $\langle \psi | \mathcal{O} | \psi \rangle$, where \mathcal{O} is defined using any subset of the l spins in the subsystem, coincides with the values obtained from the corresponding truncated GGE.

III. ALGORITHM FOR SAMPLING EIGENSTATES

For a large chain of size L , since there are $2^{L/2}$ eigenstates that are parity invariant, it is not possible to extract the local properties for each individual state in a numerical calculation. Instead, we use an unbiased sampling procedure which we detail below, to extract individual eigenstates from a microcanonical ensemble with the mean value of the energy density $e = \langle \psi | H | \psi \rangle / L$ being equal to the “target” energy density e_T and the fluctuations around the mean $\Delta e \rightarrow 0$ as $L \rightarrow \infty$. Our sampling is based on the standard algorithm for performing a microcanonical Monte-Carlo (MC) simulation introduced by Creutz [31], where an extra degree of freedom, which

we call “demon”, travels throughout the system exchanging energy with it, and changing the dynamical variables as a result.

In the context of the TFIM, we can think of the demon traveling in k space, and attempting to update the Bogoliubov fermion occupations $n_k (= 0(1))$ which fully define the eigenstate (Eqn. 6). In detail, a momentum k from the allowed positive momenta at system size L is chosen at random. Upon reaching k , the demon attempts to flip the variable n_k from $0(1)$ to $1(0)$. If this move lowers the energy of the system $E = \sum_{k>0} 2\epsilon_k(g)n_k$, this energy is then given to the demon and the flip is accepted. The demon energy, which we denote by E_D , is then updated to $E_{D'}$ as follows

$$E_D \rightarrow E_{D'} = E_D + E - E' \quad (22)$$

where E' is the new energy of the system. Note that the total energy of the system and the demon remains conserved in this process. Similarly, if the system’s energy is increased by the flip, the demon supplies that required energy and its own energy is decreased accordingly. However, to keep the demon from running off with all the energy, we restrict $E_D \geq 0$ and so only those flips are accepted for which $E_{D'} \geq 0$, otherwise the flip is rejected. This Monte-Carlo (MC) procedure thus generates an unbiased random walk in the space of configurations with $E + E_D = E_T$ since the transition $(E_D, E) \rightarrow (E_{D'}, E')$ and its reverse are allowed with equal probability. The mean energy density of the sampled energy eigenstates during the MC can be tuned to a required target energy density e_T by starting with an initial demon energy $E_D = 0$ and choosing an initial eigenstate with the appropriate energy density E_T/L . The width in the energy densities of the sampled eigenstates $\Delta e \rightarrow 0$ as $L \rightarrow \infty$ since $E_D \ll E$ as $L \gg 1$. We define one Monte-Carlo step (MCS) as $L/2$ flip attempts by the demon, and use the first 10^4 MCS as warm-up so that the memory of the initial eigenstate choice is lost, and then use the next 10^6 MCS for measurements of the individual properties of these sampled eigenstates.

IV. PROPERTIES OF TYPICAL EIGENSTATES

To understand the local properties of the *typical* eigenstates from a microcanonical ensemble with a desired mean energy density e_T at a magnetic field strength g , we sample such states using our MC and measure $\langle \psi | \sigma^x | \psi \rangle$, $\langle \psi | I_1 | \psi \rangle / L$, the distance measure $\mathcal{D}(\mathcal{C}(l), \mathcal{C}_{\text{GGE}}^{(y)}(l))$ (all of which may be readily calculated in the c fermion representation) with different choices of truncated GGEs for subsystems of l adjacent spins and the entanglement entropy $S_{ent}(l)$ of such a block for each of the generated eigenstate.

Here, we show the results of the MC for $g = 2$ with a mean energy density of $e_T = 0.3986$ (within error bars). The average demon energy $\langle E_D \rangle$ is finite and equals 3.84

(Fig. 1, inset). Firstly, we see that for large chain sizes, the sampled eigenstates have an energy density E/L which has a very narrow spread that rapidly shrinks to zero with increasing L (see Fig. 1), thus leading to an unbiased sampling of eigenstates from the microcanonical ensemble.

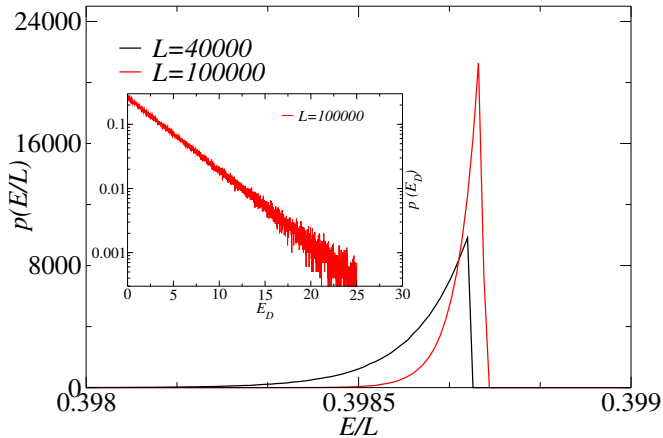


FIG. 1. Probability density of E/L for the sampled eigenstates at coupling $g = 2$ and target energy density of $e_T = 0.3986$. For the chain sizes used, the range of the sampled E/L is very small and mimics a Microcanonical ensemble. The inset shows the behaviour of the demon energy E_D during the sampling procedure.

We show the probability densities of the sampled values of $\langle \psi | \sigma^x | \psi \rangle$ and $\langle \psi | I_1 | \psi \rangle / L$ obtained from the MC in Fig. 2. The sampled values have a Gaussian distribution whose mean depends only on e_T for a given g and standard deviation that decays to zero as $L^{-1/2}$ (insets of Fig. 2). This numerical evidence strongly suggests that, in the thermodynamic limit, the local properties for any *typical* eigenstate of the TFIM (the atypical states contribute to the tails of the distributions becoming increasingly rare with increasing system size during the MC) depends *only* on the energy density e_T . Then, the natural ensemble to get the local properties correctly as $L \rightarrow \infty$ is the GE where the inverse temperature β is calculated from the mean energy density e_T , and is $\beta = 0.2604$ in this case.

This is indeed what is observed when the mean values of $\langle \psi | \sigma^x | \psi \rangle$ (Fig. 2, top panel) and $\langle \psi | I_1 | \psi \rangle / L$ (Fig. 2, bottom panel) are calculated from the sampled eigenstates. Since the width around the mean shrinks to zero when $L \rightarrow \infty$, typical eigenstates have the corresponding thermal values for $\langle \psi | \sigma^x | \psi \rangle$ and $\langle \psi | I_1 | \psi \rangle / L$ in this limit. Indeed, normal distribution of the fluctuations about the mean thermal value and the $L^{-1/2}$ scaling of the standard deviation was also observed in free models [18] and in quantities studied in Ref. 19, and may be a generic feature of many observables in typical eigenstates of integrable models at finite sizes.

It is useful to note here that that not all local operator expectation values in these typical eigenstates are

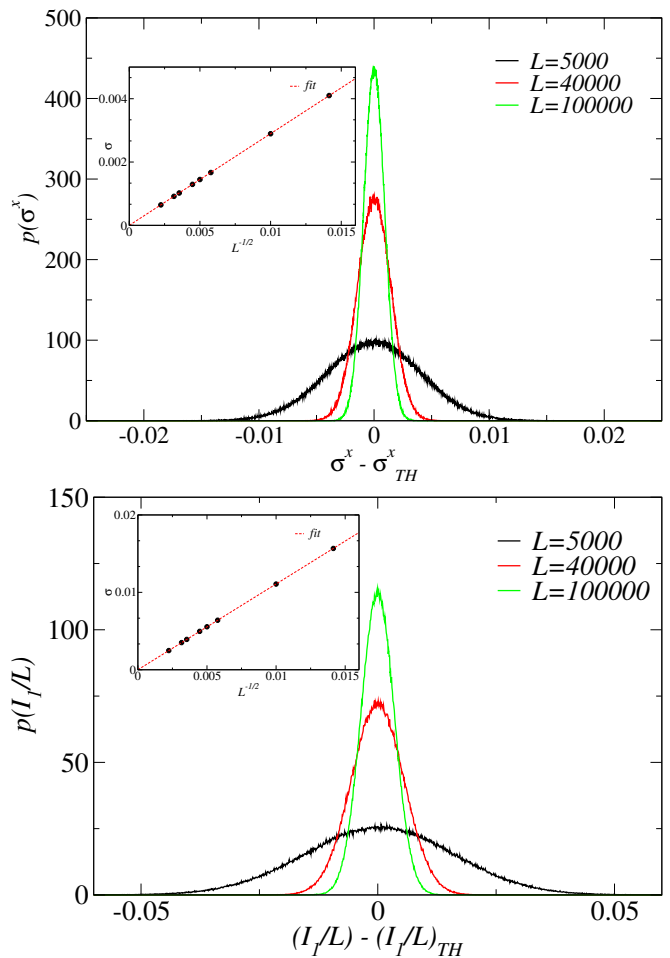


FIG. 2. Probability density generated from the sampled values of $\langle \psi | \sigma^x | \psi \rangle$ (Top panel) and $\langle \psi | I_1 | \psi \rangle / L$ (Bottom panel) for various L at $g = 2$ from within a Microcanonical ensemble with average energy density of $e_T = 0.3986$. σ_{TH} and $(I_1/L)_{TH}$ denote the corresponding thermal values at a finite β fixed only by the average energy density e_T in the thermodynamic limit. The insets of both the figures show that the standard deviation σ decreases as $L^{-1/2}$.

normally distributed about the thermal mean value at finite chain size L . E.g., we show the behaviour of the connected correlation function $G_c^{xx}(r) = \langle \psi | \sigma^x(r+1) \sigma^x(1) | \psi \rangle - \langle \psi | \sigma^x | \psi \rangle^2$ for $r = 2$ in Fig. 3, where the distribution function is clearly asymmetric (and not Gaussian about the corresponding thermal mean value) but shrinks to the thermal value again as $L \rightarrow \infty$.

To show unambiguously that the equivalence to GE holds at the level of the RDMs, which implies that

$$\rho_S = \text{Tr}_{\bar{S}} |\psi\rangle \langle \psi| = \text{Tr}_{\bar{S}} \rho_{GE} \quad (23)$$

where $\rho_{GE} = \frac{1}{Z} \exp(-\beta H)$ for a typical eigenstate $|\psi\rangle$ when $L \rightarrow \infty$ as long as the subsystem is local (i.e. $l \ll L$), we consider the behaviour of the average $\mathcal{D}(C(l), C_{GGE}^{(1)}(l))$ (where the truncated GGE with $y = 1$ coincides with GE, and we have used the inverse temperature $\beta = 0.2604$ which is fixed to give the the correct

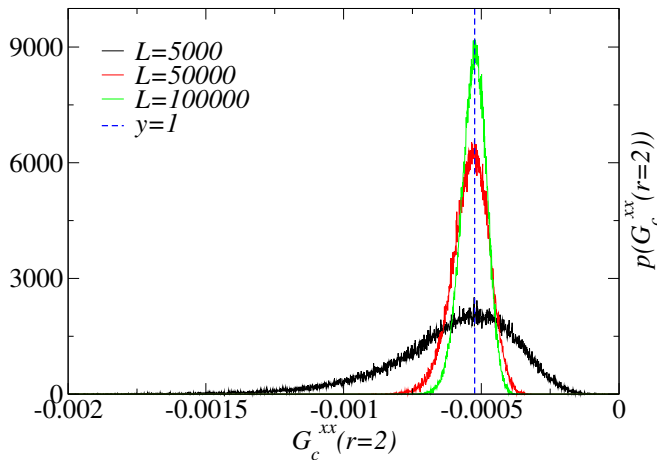


FIG. 3. Probability density generated from the sampled values of $G_c^{xx}(r) = \langle \psi | \sigma^x(r+1) \sigma^x(1) | \psi \rangle - \langle \psi | \sigma^x | \psi \rangle^2$ for $r = 2$ from within a Microcanonical shell with energy density $e_T = 0.3986$. The probability density is asymmetric about the thermal mean value but shrinks to it when $L \rightarrow \infty$.

average energy density e_T of the sampled eigenstates) and see that the distance measure itself goes to zero for the typical states as $L \rightarrow \infty$ (see Fig. 4, top panel), again as $L^{-1/2}$ at large L (we have also verified this for bigger subsystems till $l \leq 100$). This implies that *all* typical eigenstates are locally described by a GE in the thermodynamic limit. We also see that if subsystems with finite l/L are considered, then the distance measure does not go to zero as $L \rightarrow \infty$ even when l/L is very small (Fig. 4, bottom panel). This is because global operators which involve spins at a spatial separation $l \sim \mathcal{O}(L)$ cannot be described by a thermal reduced density matrix as the rest of the system cannot then act as a bath for the subsystem.

Finally, we show evidence that this feature, of typical eigenstates locally behave as if they are thermal, holds at all values of energy density e_T for the coupling $g = 2$. With our MC, we can also access eigenstates with a *negative* values of β (i.e., eigenstates which lie *above* the middle of the spectrum) by restricting the demon energy to be $E_D \leq 0$ (instead of $E_D \geq 0$) in the MC and these continue to be described by the corresponding GEs. To demonstrate the local thermal behaviour, we calculate the entanglement entropy $S_{\text{ent}}(l)$ directly from the sampled eigenstates and see that these agree very well with the corresponding thermal value of the entropy $S_{\text{TH}}(l)$ assuming a GE for the full system (see Fig. 5). Since the spectrum of the TFIM is bounded, the entanglement shows a non-monotonic behaviour with varying energy density. We have further checked that typical eigenstates at other values of the magnetic field g also behave thermally as far as local properties are concerned. Since we are considering a one-dimensional model here, such eigenstates are always paramagnetic (i.e. $\langle \psi | \sigma^z | \psi \rangle = 0$) in the thermodynamic limit for any finite energy density irrespective of the value of g .

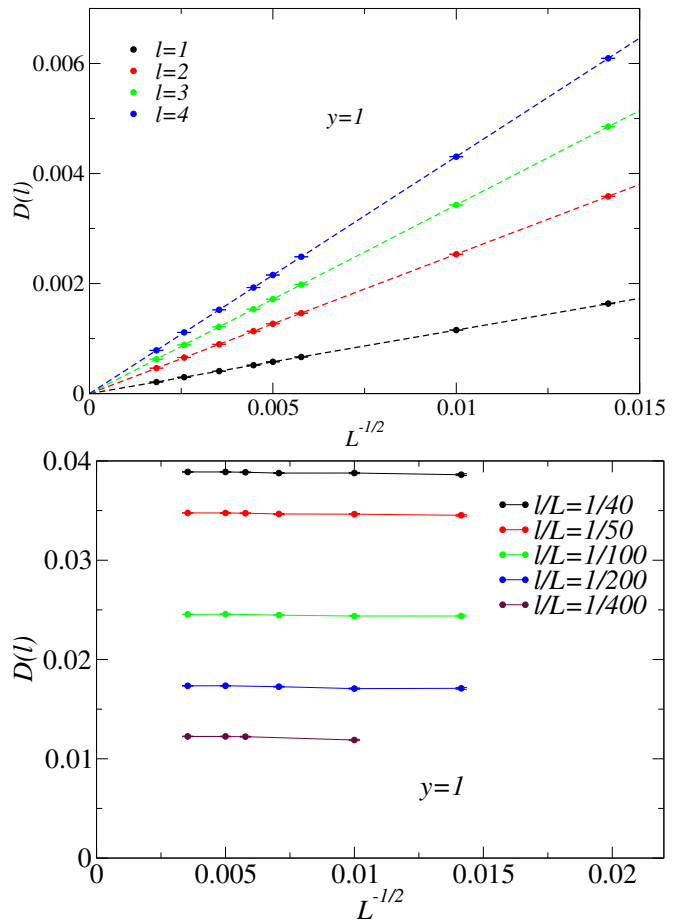


FIG. 4. (Top panel) The distance measure $\mathcal{D}(C(l), C_{\text{GGE}}^{(1)}(l)) \rightarrow 0$ as $L \rightarrow \infty$ when $l \ll L$ implying that the local RDMs are thermal. This is however not the case when subsystems with finite l/L are considered (Bottom panel).

The thermal behaviour of the local observables in the typical eigenstates of the TFIM in the thermodynamic limit can be related to an analogous behaviour of the Bogoliubov fermion occupation n_k which determine the densities of *all* the (local) conserved quantities of the model (Eqn. 12). When $L \rightarrow \infty$, we get

$$\frac{I_n}{L} = \frac{1}{\pi} \int_0^\pi \cos(nk) \epsilon(k) n_c(k) \quad (24)$$

where the momentum k becomes a continuous variable and $n_c(k) \in [0, 1]$ represents the average occupation of the Bogoliubov fermions at momentum k .

For free fermions, it was demonstrated in Ref. 32 (see also Refs. 33 and 34) that if a ‘‘coarse-grained’’ occupation number $n_c(k)$, defined through some suitable averaging procedure of the microscopic variables n_k in a shell of (infinitesimal) width δk around k is considered, then the most probable form of $n_c(k)$ appears thermal (i.e. the Fermi-Dirac distribution for free fermions) by the standard entropy maximization argument. Clearly, many different microscopic realizations of $n_k = 0, 1$ can

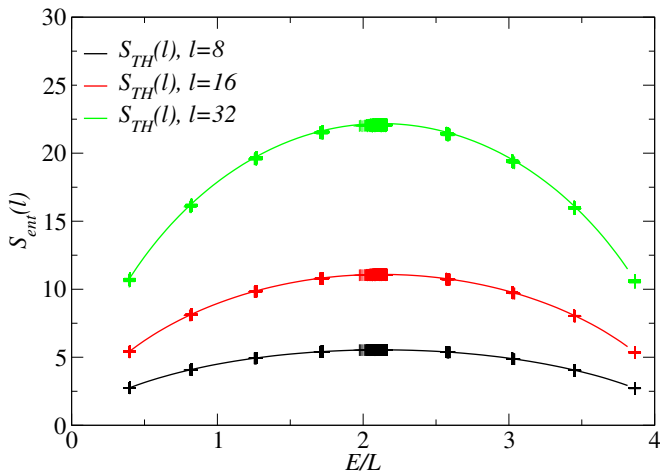


FIG. 5. The entanglement entropy of small subsystems of size l , denoted by $S_{\text{ent}}(l)$, obtained from the typical eigenstates sampled at different energy densities E/L at coupling $g = 2$ for a chain size of $L = 5000$. These match very well with the corresponding thermal entropy $S_{\text{TH}}(l)$ obtained from the average energy density of the sampled eigenstates.

give the same “coarse-grained” $n_c(k)$ in the thermodynamic limit, which explains the resulting thermal values of the densities, I_n/L , for the typical eigenstates as $L \rightarrow \infty$ (Fig. 2). For a finite system size of L , there are $\mathcal{O}(\delta k L)$ momentum modes in a shell of width δk around k , and hence fluctuations of $\mathcal{O}(1/\sqrt{L})$ that are normally distributed around the most probable $n_c(k)$ can be expected for typical eigenstates by the Central Limit Theorem. This explains the normal distribution of $\langle \psi | \sigma^x | \psi \rangle$ and $\langle \psi | I_1 | \psi \rangle / L$ about the corresponding thermal values at finite L (Fig. 2) since these quantities depend linearly on the fermion occupation.

V. SAMPLING ATYPICAL EIGENSTATES

The demon algorithm can be easily generalized to generate atypical eigenstates from within the Microcanonical ensemble that do not satisfy GE. These states are characterized by *athermal* values of the densities I_n/L and there is again a large number of such eigenstates ($\mathcal{O}(e^L)$) for a chain of size L . We adapt our algorithm to sample energy eigenstates from within a truncated *generalized* Microcanonical ensemble defined by $(E/L, I_1/L, \dots)$ where the densities of the other integrals of motion $(I_1/L, \dots)$ are set to be significantly different from their corresponding thermal values in the thermodynamic limit. Such eigenstates can clearly not be described by a GE locally. Here, we discuss our results for *typical* eigenstates from within the simplest (truncated) generalized Microcanonical ensemble $(E/L, I_1/L)$ and the extension to other cases is immediate.

For sampling such rare eigenstates, we now endow the demon with two properties E_D and $(I_1)_D$. The demon

again visits a momentum k randomly from the allowed positive momenta at system size L and attempts to flip the variable n_k from 0(1) to 1(0). The demon variables E_D and $(I_1)_D$ are simultaneously updated as

$$\begin{aligned} E_D &\rightarrow E_{D'} = E_D + E - E' \\ (I_1)_D &\rightarrow (I_1)_{D'} = (I_1)_D + I_1 - I_1' \end{aligned} \quad (25)$$

where $E = \sum_{k>0} 2\epsilon_k n_k$ and $I_1 = \sum_{k>0} 2\epsilon_k n_k \cos(k)$ as defined earlier, and E' and I_1' are the correspondingly values after the flip. We further restrict the demon to have $E_D \geq 0$ and $(I_1)_D \geq 0$ at all times and only those flips which satisfy these conditions simultaneously are accepted, otherwise the flip attempt is aborted and another k is chosen at random. We choose the initial seed eigenstate with appropriate values of E_T and $(I_1)_T$ and initialize $E_D, (I_1)_D = 0$. Since the MC conserves $E + E_D = E_T$ and $I_1 + (I_1)_D = (I_1)_T$ and in a large system, since $E_D \ll E$ and $(I_1)_D \ll I_1$, we therefore only sample eigenstates with a fixed energy per site *and* a fixed density $(I_1)/L$ when $L \rightarrow \infty$. Here, we show sampling of eigenstates at $g = 2$ with the same $E/L = 0.3986$ as in the previous section but now with a very atypical value of $(I_1)/L = -0.093$ (Fig. 6) which is far from the corresponding thermal value of $(I_1/L)_{\text{TH}} = +0.075$ given the energy density.

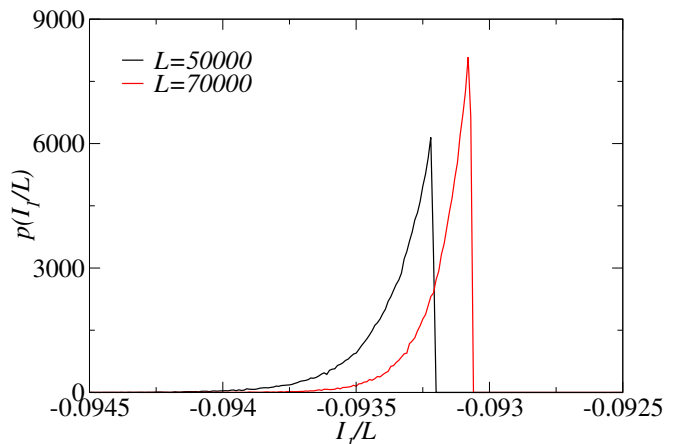


FIG. 6. Probability density of $(I_1)/L$ for the sampled eigenstates when the demon has both E_D and $(I_1)_D$ as its properties at the same target energy density $e_T = 0.3986$ at $g = 2$ as in Fig. 1 but with very different I_1/L compared to the corresponding thermal value of $(I_1/L)_{\text{TH}} = 0.075$.

For the typical eigenstates generated in this generalized Microcanonical ensemble, we clearly see that the RDMs *cannot* be described with corresponding GEs, unlike in the previous case (Fig. 7, top panel) since now the distance measure does not go to zero with $y = 1$. However, the truncated GGE with $y = 2$ (i.e. with the athermal density of I_1 taken into account through λ_1), which gives $\beta = 0.296$ and $\lambda_1 = 0.129$, exactly describes the local properties of these sampled eigenstates in the thermodynamic limit when $l \ll L$ (Fig. 7, bottom panel).

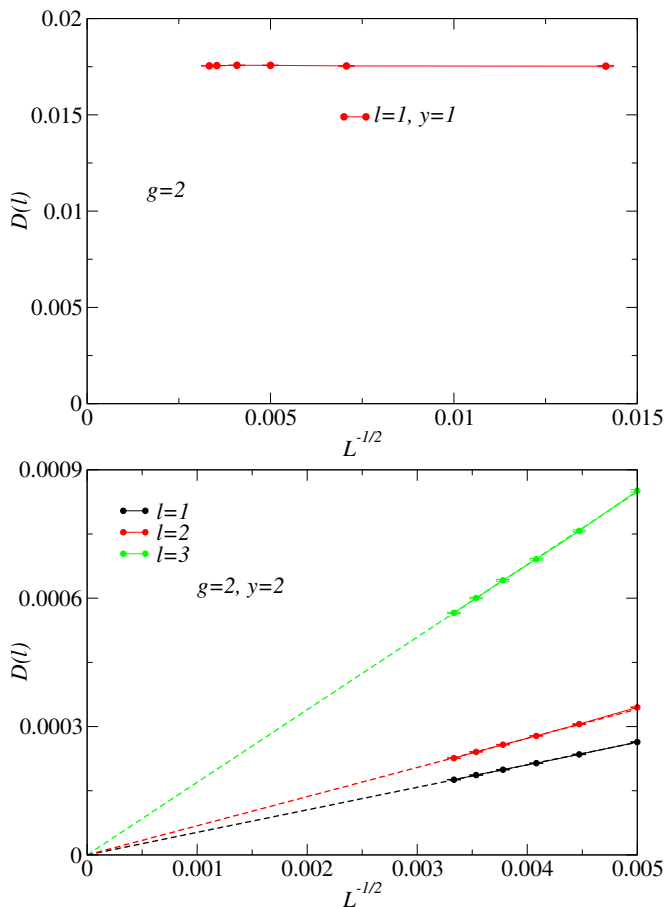


FIG. 7. The local properties of *typical* eigenstates with $E/L = 0.3986$ and $(I_1/L) = -0.093$ at $g = 2$ (which is very different from $(I_1/L)_{\text{TH}} = +0.075$) are not described by a GE in the thermodynamic limit (Top panel), but by a $y = 2$ truncated GGE with $\beta = 0.296$ and $\lambda_1 = 0.129$ (Bottom panel).

Using the basic definition of entropy $S = \log(\Omega)$, where Ω denotes the number of eigenstates that share the same local properties, we thus see that the probability of encountering an eigenstate which is described by a $y = 2$ ensemble characterized by $(E/L, I_1/L)$ (where I_1/L is athermal) versus an eigenstate described by a GE characterized by E/L alone equals $\exp[-L\{s(E/L) - s(E/L, I_1/L)\}]$, where $s(E/L)$ is the entropy density of the system at inverse temperature β fixed by E/L and $s(E/L, I_1/L)$ is the corresponding entropy density for the system described by a $y = 2$ truncated GGE, with (β, λ_1) fixed jointly by $(E/L, I_1/L)$. This quantifies why such athermal eigenstates are “rare” states in the TFIM, even though their number still scales exponentially with system size.

Similarly, we have numerically verified that a *typical* energy eigenstate from other generalized Microcanonical ensembles with the first $m + 1$ local conservation laws specified is completely characterized (as far as all local properties are concerned) by a suitable truncated GGE with only $y = m + 1$ as $L \rightarrow \infty$. This behaviour

in the thermodynamic limit can be argued from the corresponding most probable distribution of the coarse-grained (in momentum space) Bogoliubov fermions occupations $n_c(k)$ (Eqn. 24) by extending the arguments of Ref. 32, taking into account the additional conservation laws which specify the generalized Microcanonical ensembles in terms of the Bogoliubov fermion occupations n_k .

A. Truncated GGE for an arbitrary eigenstate

For typical eigenstates drawn from generalized Microcanonical ensembles in the TFIM, we have demonstrated that only a *few* Lagrange multipliers are necessary for describing all the local properties of the state in a thermodynamically large system and all other Lagrange multipliers can be set to zero. E.g. a GE with only $\lambda_0 = \beta$ being non-zero, and all other Lagrange multipliers $\lambda_n = 0$, provides the description for all local properties for typical eigenstates drawn from a Microcanonical ensemble as shown in Sec. IV. What about eigenstates where the Lagrange multipliers λ_n *cannot* be set to be zero beyond a certain n and a full GGE description is therefore necessary? These eigenstates nonetheless have a finite energy density E/L and show a volume law behaviour for the entanglement entropy and we study the RDMs of these states in this section. These eigenstates are generated by ensuring that the coarse-grained (in momentum space) Bogoliubov fermion occupation $n_c(k)$ is a *discontinuous* function of k in the thermodynamic limit. There are several ways to achieve this and most simply, these eigenstates are obtained by placing the Bogoliubov fermion occupations $n_k = 0(1)$ with probability $1 - p_1(p_1)$ in the first $L/2$ positive k modes and with a different probability $1 - p_2(p_2)$ in the next $L/2$ modes. For a large chain size L , any typical realization of this random process of placing $n_k = 0(1)$ generates an energy eigenstate where the coarse-grained $n_c(k)$ is p_1 for $0 \leq k \leq \pi/2$, and p_2 for $\pi/2 \leq k \leq \pi$. The discontinuity in $n_c(k)$ then leads to a slow decay of $|\lambda_n|$ as $1/n$ (see Fig. 8 (Top panel)) for any $p_1 \neq p_2$. In Fig. 8 (Bottom panel), we show the results of the comparison of the RDMs for such an atypical eigenstate in a chain size of $L = 2000$, where we take $p_1 = 0.1$ and $p_2 = 0.4$, with various truncated GGEs.

Even though the full GGE is required if we need the accurate description of *all* local properties for such eigenstates in the thermodynamic limit, we clearly see that depending on the subsystem size l being considered, one still requires only the first $y \sim l$ most local conservation laws for an “accurate” description of the properties of even such eigenstates and not *all* the integrals of motion from the behaviour of the distance measure $D(l)$ (Fig. 8, bottom panel). Going to bigger subsystems requires specifying a larger number (y) of integrals of motion to reduce $D(l)$. However, even for such eigenstates, we see that the most local integrals of motion play the most important role in describing local properties, and this constitutes the “eigenstate thermalization version”

of a similar conclusion reached in Ref. 25 for steady states following quantum quenches in the 1D TFIM.

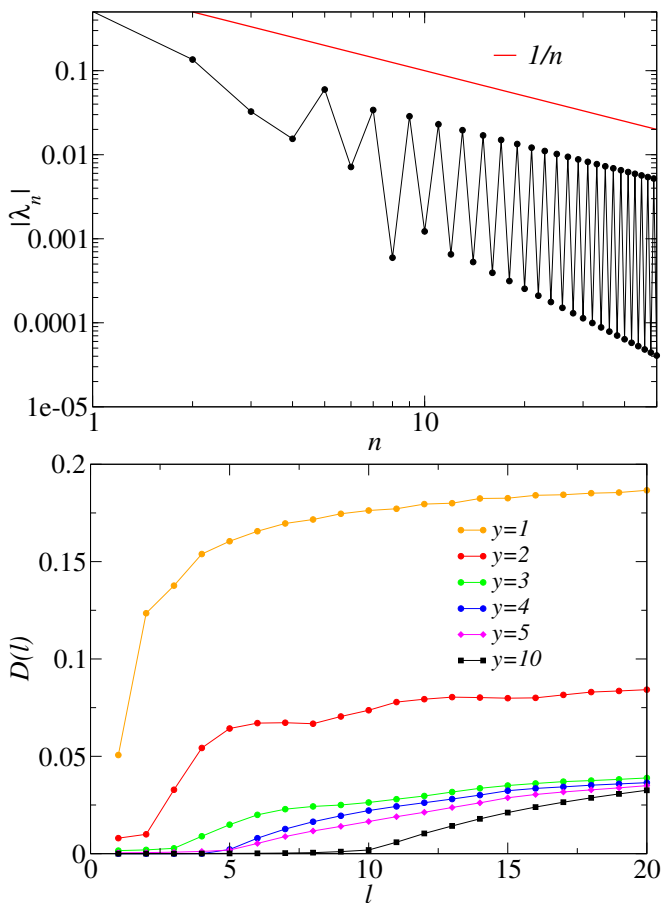


FIG. 8. (Top panel) The decay of $|\lambda_n|$ as a function of n in an eigenstate where the coarse-grained $n_c(k)$ is discontinuous in the thermodynamic limit with $p_1 = 0.1$ and $p_2 = 0.4$. (Bottom panel) Results for the distance measure $D(l)$ for such a highly atypical eigenstate generated with $p_1 = 0.1$ and $p_2 = 0.4$ for a chain size of $L = 2000$ as a function of l with different truncated GGEs.

VI. QUENCH FROM A TYPICAL EIGENSTATE

We now address the situation when the Hamiltonian is time-dependent and consider the simplest case of a quantum quench, where the magnetic field (g) is suddenly changed from a pre-quench to a post-quench value at $t = 0$. Typically, when considering quantum quenches, the starting state is assumed to be the ground state of the pre-quench Hamiltonian. Here, we consider the case where the initial state is instead a typical excited eigenstate of the pre-quench Hamiltonian (see also Ref. 24). Since such initial states are locally thermal as we explicitly showed in the previous sections, a natural question is whether the unitary dynamics following the quantum quench at $t = 0$ keeps them thermal at long times.

We will show here that this is not the case since such states do not have a finite overlap with the typical eigenstates of the post-quench Hamiltonian but only with its rare eigenstates in the thermodynamic limit. However, if the initial state was an eigenstate of a non-integrable model, the final steady state might appear thermal [35]. Thus, the long time description of the steady state again requires a GGE but there are important differences when compared to a ground state quench.

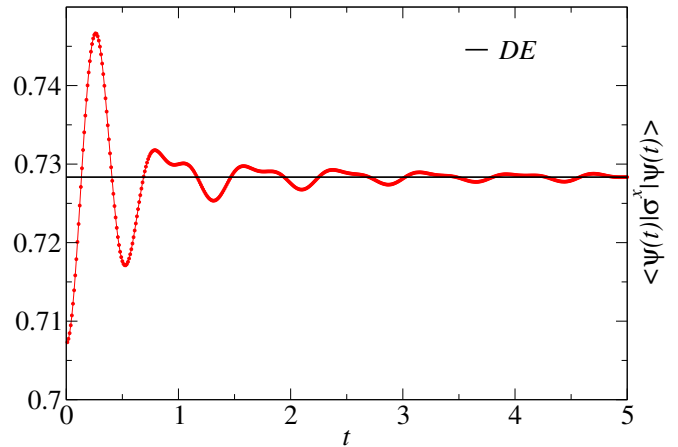


FIG. 9. The time evolution of the expectation value of the local operator σ^x where the starting state at $t = 0$ is a typical eigenstate (generated from the demon algorithm) at the coupling $g_i = 2$ and chain size $L = 30000$. The system's magnetic field is quenched to $g_f = 3$ at $t = 0$ and the unitary dynamics of the state leads to the Diagonal ensemble at long time (but smaller than the revival time of the finite system).

The density matrix of the full system at a finite time can be written formally as

$$\begin{aligned} \rho(t) &= |\psi(t)\rangle\langle\psi(t)| \\ &= \sum_i |\langle\psi_i^f|\psi(0)\rangle|^2 |\psi_i^f\rangle\langle\psi_i^f| \\ &+ \sum_{i_1 \neq i_2} e^{-i(E_{i_1}^f - E_{i_2}^f)t} \langle\psi_{i_1}^f|\psi(0)\rangle\langle\psi(0)|\psi_{i_2}^f\rangle |\psi_{i_1}^f\rangle\langle\psi_{i_2}^f| \end{aligned} \quad (26)$$

where $|\psi_i^f\rangle$ represent the eigenstates of the post-quench Hamiltonian, E_i^f its energy and $|\psi(0)\rangle$ denotes the starting state at $t = 0$. In the thermodynamic limit, the $i_1 \neq i_2$ terms cancel each other out when $t \rightarrow \infty$ [4, 12] and hence, the density matrix of the steady state of the system coincides with the Diagonal ensemble (DE), described by the time-independent density matrix ρ_{DE} :

$$\rho_{\text{DE}} = \sum_i |\langle\psi_i^f|\psi(0)\rangle|^2 |\psi_i^f\rangle\langle\psi_i^f|. \quad (27)$$

In a finite system, any local operator will show revivals but this time scale becomes progressively larger and diverges [36] as $L \rightarrow \infty$.

The time-dependent wavefunction $|\psi(t)\rangle = \otimes_{k>0} |\psi_k(t)\rangle$ for the quench, where $|\psi_k(t)\rangle = U_k^n(t)c_k^\dagger c_{-k}^\dagger |0\rangle + V_k^n(t)|0\rangle$, can be easily worked out

for $t > 0$, by expressing the $t = 0^-$ state at each k in terms of the $(U_{k0(1)}(g_f), V_{k0(1)}(g_f))$ at the new coupling g_f . Doing this, we obtain $U_k^n(t)$ and $V_k^n(t)$ as follows:

$$\begin{aligned} \begin{pmatrix} U_k^0(t) \\ V_k^0(t) \end{pmatrix} &= +e^{+i\epsilon_k(g_f)t} \cos((\theta_k^i - \theta_k^f)/2) \begin{pmatrix} U_{k0}(g_f) \\ V_{k0}(g_f) \end{pmatrix} + e^{-i\epsilon_k(g_f)t} \sin((\theta_k^i - \theta_k^f)/2) \begin{pmatrix} U_{k1}(g_f) \\ V_{k1}(g_f) \end{pmatrix} \\ \begin{pmatrix} U_k^1(t) \\ V_k^1(t) \end{pmatrix} &= -e^{+i\epsilon_k(g_f)t} \sin((\theta_k^i - \theta_k^f)/2) \begin{pmatrix} U_{k0}(g_f) \\ V_{k0}(g_f) \end{pmatrix} + e^{-i\epsilon_k(g_f)t} \cos((\theta_k^i - \theta_k^f)/2) \begin{pmatrix} U_{k1}(g_f) \\ V_{k1}(g_f) \end{pmatrix} \end{aligned} \quad (28)$$

with the $n = 0(1)$ index in $U_k^n(t)$ and $V_k^n(t)$ denoting whether the $t = 0^-$ eigenstate at $g = g_i$ is $(U_{kn}(g_i), V_{kn}(g_i))$ at momentum k , and θ_k^i, θ_k^f denote the Bogoliubov angles θ_k^g (see Eq. 7) for the pre-quench (g_i) and post-quench (g_f) values of the magnetic field respectively. We show the result of $\langle \psi(t) | \sigma^x | \psi(t) \rangle$ for a typical eigenstate at $g_i = 2$ generated from the demon algorithm with $e_T = 0.3986$ where the magnetic field is quenched to $g_f = 3$ at $t = 0$ in Fig. 9. We see that that $\langle \psi(t) | \sigma^x | \psi(t) \rangle$ already converges close to the DE result after a relatively short time $t \sim 5$.

We next calculate the steady state values of local observables $\langle H(g_f) \rangle / L$, $\langle I_1(g_f) \rangle / L$ and $\langle \sigma^x \rangle$ given that the quench starts from each of the sampled eigenstates from the MC (with $g_i = 2$ and $e_T = 0.3986$) at $t = 0$ using the appropriate DE determined by the initial state at g_i and the value of g_f and show the probability distributions of these steady state quantities in Fig. 10.

The distributions of the DE values for the quantities shown in Fig. 10 are normally distributed and the standard deviation progressively shrinks to zero as L is increased, which implies that in the thermodynamic limit, quenches originating from *any* typical eigenstate characterised by the same initial energy density e_T at coupling g_i lead to steady states which are identical as far as local properties are concerned. However, the mean values of the steady state distributions of $\langle I_1(g_f) \rangle / L$ (Fig. 10, Top panel) and $\langle \sigma^x \rangle$ (Fig. 10, Bottom panel) are very different from the expected GE results fixed by the mean energy density of the final post-quench Hamiltonian (see inset of Top panel in Fig. 10). Thus the steady state obtained after a quantum quench from a typical eigenstate of the pre-quench Hamiltonian is not thermal and further conservation laws are needed for a quantitative agreement.

We now detail the construction of the GGE in the thermodynamic limit, and give the analytic expression for the Lagrange multipliers λ_n . The mean of the probability distributions of the different quantities shown in Fig. 10 ($\langle H(g_f) \rangle / L$, $\langle I_1(g_f) \rangle / L$ and $\langle \sigma^x \rangle$) are all correctly captured by this GGE, and provides strong numerical support for its correctness in the thermodynamic limit.

After a quench, the average Bogoliubov fermion number $\langle n_k^{i,f} \rangle$ at each k is conserved (and thus does not change as a function of t) because of the form of the

post-quench Hamiltonian. Then, we have

$$\langle n_k^{i,f} \rangle = (p) \sin^2 \left(\frac{\theta_k^i - \theta_k^f}{2} \right) + (1-p) \cos^2 \left(\frac{\theta_k^i - \theta_k^f}{2} \right) \quad (29)$$

where $p = 0(1)$ if $n_k(g_i) = 0(1)$ for the eigenstate of g_i at $t = 0$. In the thermodynamic limit, all the microscopic $n_k(g_i)$ lead to the same coarse-grained $n_c(k)$ which follows a thermal distribution that is fixed only by the average energy density of the eigenstate. Thus, when $L \rightarrow \infty$, we can replace the p variables (which equal $n_k(g_i)$ microscopically) by the same thermal distribution to get its coarse-grained version:

$$p_c(k) = \frac{\exp(-\beta \epsilon_k^i)}{\exp(-\beta \epsilon_k^i) + \exp(+\beta \epsilon_k^i)} \quad (30)$$

where β is the inverse temperature of the GE that describes the local properties of the typical eigenstates at g_i . Thus, in the $L \rightarrow \infty$ limit, we obtain

$$\langle n_k^{i,f} \rangle = \frac{e^{-\beta \epsilon_k^i} \cos^2 \left(\frac{\theta_k^i - \theta_k^f}{2} \right) + e^{\beta \epsilon_k^i} \sin^2 \left(\frac{\theta_k^i - \theta_k^f}{2} \right)}{e^{-\beta \epsilon_k^i} + e^{\beta \epsilon_k^i}} \quad (31)$$

The Lagrange multipliers λ_n wrt the final post-quench Hamiltonian (at g_f) are then defined by using Eqn. 11 and Eqn. 16:

$$\begin{aligned} \lambda_n &= \frac{2 - \delta_{n,0}}{\pi} \int_0^\pi \cos(nk) \mathcal{F}(g_i, g_f, \beta, k) \\ \mathcal{F}(g_i, g_f, \beta, k) &= \frac{1}{2\epsilon_k^f} \log \left(\frac{1 - \langle n_k^{i,f} \rangle}{\langle n_k^{i,f} \rangle} \right) \end{aligned} \quad (32)$$

Thus, knowing the initial energy density of the typical eigenstate at the pre-quench magnetic field value of g_i , and the couplings g_i and g_f , completely fixes the Lagrange multipliers (λ_n) and hence the GGE from Eqn. 15. The values obtained from this GGE are fully consistent with the mean values of $\langle H(g_f) \rangle / L$, $\langle I_1(g_f) \rangle / L$, σ^x in the steady state around which the standard deviation shrinks to zero as $L \rightarrow \infty$ in Fig. 10. At low β , this expression can be further simplified to give

$$\lambda_n = \left(\frac{2 - \delta_{n,0}}{\pi} \right) \beta \int_0^\pi \left(\frac{\epsilon_k^i}{\epsilon_k^f} \cos(\theta_k^i - \theta_k^f) \right) \cos(nk) \quad (33)$$

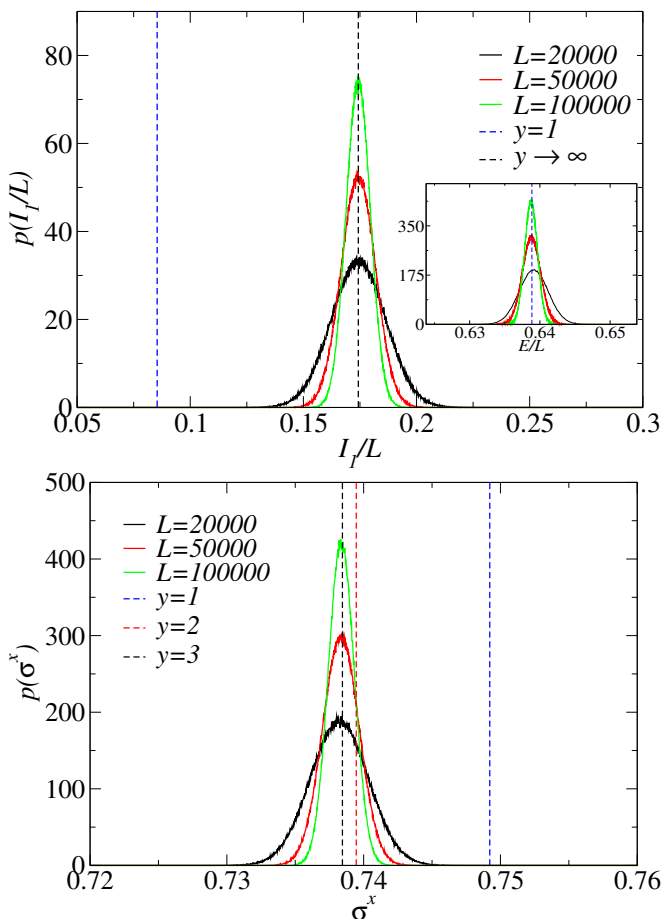


FIG. 10. (Top panel) The probability density of $\langle I_1(g_f) \rangle / L$ obtained from the steady state of the system starting from typical eigenstates at chain size L and at coupling $g_i = 2$ and quenched to a post-quench coupling of $g_f = 3$. The inset shows the corresponding probability density for $\langle H(g_f) \rangle / L$ in the steady state. (Bottom panel) The corresponding probability density of $\langle \sigma^x \rangle$ in the steady state. Clearly, the system's steady state is no longer described by a GE after the quench.

Clearly, only when $\beta = 0$ for the initial pre-quench eigenstate is the final steady state also thermal (with $\beta = 0$ again) with respect to the final post-quench Hamiltonian. Even at small β , λ_n for $n > 0$ are non-zero (though small) and hence one obtains a GGE for the steady state. The athermal nature of the ensemble is related to the athermal behaviour of $\langle n_k^{i,f} \rangle$ (Eqn. 29), which fixes all the (local) conserved quantities, since it cannot be expressed as $\exp(-\beta_f \epsilon_k(g_f)) / (\exp(+\beta_f \epsilon_k(g_f)) + \exp(-\beta_f \epsilon_k(g_f)))$ for any β_f as long as the initial $\beta \neq 0$.

Note that the λ_n when the initial state is the ground state of the pre-quench Hamiltonian can be simply obtained by taking $\beta \rightarrow \infty$ and matches the results obtained in that context by Fagotti and Essler [25]. From this previous work, it is known that λ_n decay rather slowly with distance as $1/n$ when the $t = 0$ state is the pre-quench Hamiltonian's ground state, because of the

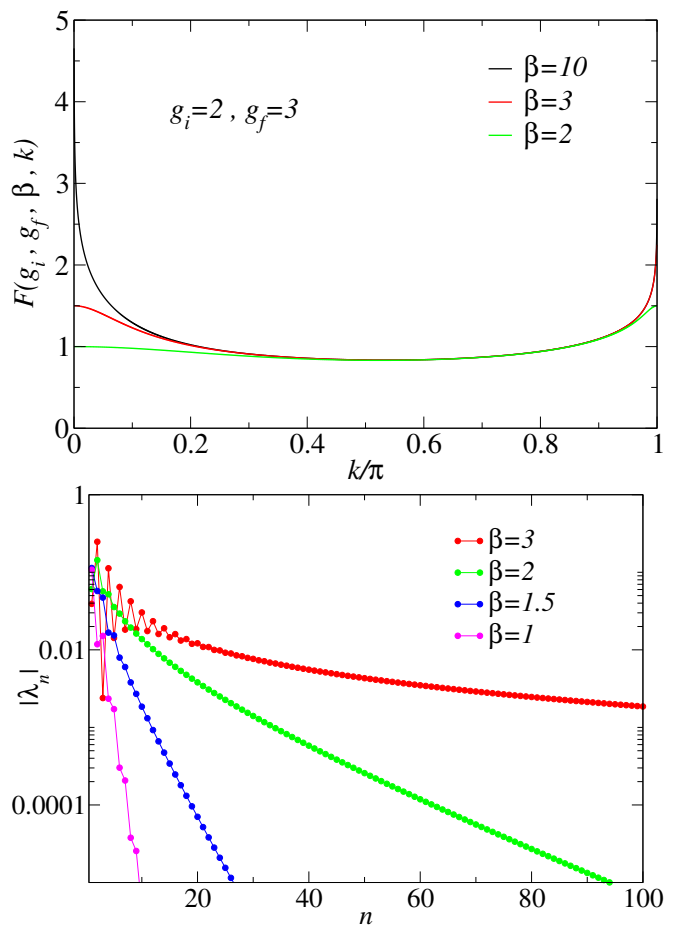


FIG. 11. (Top panel) The singularities present in $\mathcal{F}(g_i, g_f, \beta \rightarrow \infty, k)$ at $k = 0, \pi$ get rounded off at finite β that corresponds to the energy density of a typical (pre-quench Hamiltonian's) eigenstate. (Bottom panel) The decay of the Lagrange multipliers for the post-quench GGE as a function of distance n . Here, $g_i = 2$, $g_f = 3$ and β is fixed only by the energy density of the typical eigenstate of the pre-quench Hamiltonian.

logarithmic singularity of $\mathcal{F}(g_i, g_f, \beta \rightarrow \infty, k)$ at $k = 0$ and $k = \pi$. However, for any finite β (which corresponds to a highly excited eigenstate at $t = 0$), the singularities are rounded off as shown in Fig. 11 (Top panel). This instead leads to an exponential decay of $|\lambda_n| \sim \exp(-n/\xi)$ as shown in Fig. 11 (Bottom panel), where ξ indicates the length-scale associated with the exponential decay in n . It will be interesting to obtain an analytic expression for ξ as a function of β, g_i, g_f .

VII. CONCLUSIONS

We have studied the reduced density matrices and local properties of highly excited eigenstates of the transverse field Ising chain, sampling them using an unbiased Monte-Carlo technique. We find that, in spite of being integrable with an extensive number of conserved quan-

tities, typical high energy eigenstates are described by a finite temperature Gibbs ensemble for all local properties in the thermodynamic limit. Our sampling method also allows us exploring rare (athermal) eigenstates, and we explicitly demonstrate that such states are locally described by appropriate truncated Generalized Gibbs ensembles with only a few non-zero Lagrange multipliers. We also consider a class of high energy eigenstates for which the full GGE is required to describe local properties accurately. Nonetheless, the most local conservation laws still play the most important role in describing local properties. We, however, show that even for a quantum quench from a typical high-energy eigenstate of the pre-quench Hamiltonian, the resulting steady state requires a full GGE description. Our study leaves many open is-

ues for future studies. For example, it will be interesting to investigate the behaviour of unequal time correlation functions of high energy excited states, especially in light of the results presented in Ref. 37. Another interesting question is whether this picture of typicality holds for free Hamiltonians with long range interactions. A related question is regarding the typical nature of the periodic Gibbs' ensemble [13] produced by driving free-fermions (or other integrable models mapable to that) periodically: if we observe the asymptotic synchronized state stroboscopically, do we typically get a thermal state? The question is interesting, since the effective Floquet hamiltonian, though still bilinear in fermions, may be long-ranged, and can often be non-local in terms of the original degrees of freedom.

-
- [1] L. D. Landau and E. M. Lifshitz, *Course of Theoretical Physics: Statistical Physics, Part 1*, Vol. 5 (Elsevier, 2013)
- [2] M. Srednicki, Phys. Rev. E **50**, 888 (Aug 1994), <http://link.aps.org/doi/10.1103/PhysRevE.50.888>
- [3] J. M. Deutsch, Phys. Rev. A **43**, 2046 (Feb 1991), <http://link.aps.org/doi/10.1103/PhysRevA.43.2046>
- [4] M. Rigol, V. Dunjko, and M. Olshanii, Nature **452**, 854 (April 2008), http://www.nature.com/nature/journal/v452/n7189/supinfo/nature06838_S1.html
- [5] L. D'Álessio, Y. Kafri, A. Polkovnikov, and M. Rigol(2015), arXiv:1509.06411
- [6] J. V. Neumann, *Mathematical Foundations of Quantum Mechanics* (Princeton University Press, 1955)
- [7] S. Suzuki, J. Inoue, and B. K. Chakrabarti, *Quantum Ising Phases and Transitions in Transverse Ising Models* (Springer, Heidelberg, 2013)
- [8] S. Sachdev, *Quantum Phase Transitions* (Cambridge University Press, 2011)
- [9] E. T. Jaynes, Phys. Rev. **106**, 620 (May 1957), <http://link.aps.org/doi/10.1103/PhysRev.106.620>
- [10] M. Rigol, V. Dunjko, V. Yurovsky, and M. Olshanii, Phys. Rev. Lett. **98**, 050405 (Feb 2007), <http://link.aps.org/doi/10.1103/PhysRevLett.98.050405>
- [11] A. C. Cassidy, C. W. Clark, and M. Rigol, Phys. Rev. Lett. **106**, 140405 (Apr 2011), <http://link.aps.org/doi/10.1103/PhysRevLett.106.140405>
- [12] J.-S. Caux and F. H. L. Essler, Phys. Rev. Lett. **110**, 257203 (Jun 2013), <http://link.aps.org/doi/10.1103/PhysRevLett.110.257203>
- [13] A. Lazarides, A. Das, and R. Moessner, Phys. Rev. Lett. **112**, 150401 (2014)
- [14] P. Calabrese and J. Cardy, Phys. Rev. Lett. **96**, 136801 (Apr 2006), <http://link.aps.org/doi/10.1103/PhysRevLett.96.136801>
- [15] C. Kollath, A. M. Läuchli, and E. Altman, Phys. Rev. Lett. **98**, 180601 (Apr 2007), <http://link.aps.org/doi/10.1103/PhysRevLett.98.180601>
- [16] A. Polkovnikov, K. Sengupta, A. Silva, and M. Vengalattore, Rev. Mod. Phys. **83**, 863 (Aug 2011)
- [17] S. Goldstein, J. L. Lebowitz, R. Tumulka, and N. Zanghì, Phys. Rev. Lett. **96**, 050403 (Feb 2006), <http://link.aps.org/doi/10.1103/PhysRevLett.96.050403>
- [18] G. Biroli, C. Kollath, and A. M. Läuchli, Phys. Rev. Lett. **105**, 250401 (Dec 2010), <http://link.aps.org/doi/10.1103/PhysRevLett.105.250401>
- [19] V. Alba, Phys. Rev. B **91**, 155123 (Apr 2015), <http://link.aps.org/doi/10.1103/PhysRevB.91.155123>
- [20] T. N. Ikeda, Y. Watanabe, and M. Ueda, Phys. Rev. E **87**, 012125 (Jan 2013), <http://link.aps.org/doi/10.1103/PhysRevE.87.012125>
- [21] L. F. Santos and M. Rigol, Phys. Rev. E **82**, 031130 (Sep 2010), <http://link.aps.org/doi/10.1103/PhysRevE.82.031130>
- [22] H. Kim, T. N. Ikeda, and D. A. Huse, Phys. Rev. E **90**, 052105 (Nov 2014), <http://link.aps.org/doi/10.1103/PhysRevE.90.052105>
- [23] W. Beugeling, R. Moessner, and M. Haque, Phys. Rev. E **89**, 042112 (Apr 2014), <http://link.aps.org/doi/10.1103/PhysRevE.89.042112>
- [24] L. Bucciantini, M. Kormos, and P. Calabrese, Journal of Physics A: Mathematical and Theoretical **47**, 175002 (2014), <http://stacks.iop.org/1751-8121/47/i=17/a=175002>
- [25] M. Fagotti and F. H. L. Essler, Phys. Rev. B **87**, 245107 (Jun 2013), <http://link.aps.org/doi/10.1103/PhysRevB.87.245107>
- [26] G. Vidal, J. I. Latorre, E. Rico, and A. Kitaev, Phys. Rev. Lett. **90**, 227902 (Jun 2003), <http://link.aps.org/doi/10.1103/PhysRevLett.90.227902>
- [27] P. Calabrese, F. H. L. Essler, and M. Fagotti, Phys. Rev. Lett. **106**, 227203 (Jun 2011)
- [28] P. Calabrese, F. H. L. Essler, and M. Fagotti, J. Stat. Mech., P07016(2012)
- [29] M.-C. Chung and I. Peschel, Phys. Rev. B **64**, 064412 (Jul 2001), <http://link.aps.org/doi/10.1103/PhysRevB.64.064412>
- [30] A. Sen and K. Sengupta(2015), arXiv:1511.03668
- [31] M. Creutz, Phys. Rev. Lett. **50**, 1411 (May 1983), <http://link.aps.org/doi/10.1103/PhysRevLett.50.1411>
- [32] H.-H. Lai and K. Yang, Phys. Rev. B **91**, 081110 (Feb 2015), <http://link.aps.org/doi/10.1103/PhysRevB.91.081110>
- [33] M. Storms and R. R. P. Singh, Phys. Rev. E **89**, 012125 (Jan 2014), <http://link.aps.org/doi/10.1103/PhysRevE.89.012125>

- [34] X. Li, J. Pixley, D.-L. Deng, S. Ganeshan, and S. D. Sarma(2016), arXiv:1602.01849
- [35] M. Rigol and M. Srednicki, Phys. Rev. Lett. **108**, 110601 (Mar 2012), <http://link.aps.org/doi/10.1103/PhysRevLett.108.110601>
- [36] J. Häppölä, G. B. Halász, and A. Hamma, Phys. Rev. A **85**, 032114 (Mar 2012), <http://link.aps.org/doi/10.1103/PhysRevA.85.032114>
- [37] L. Maldacena, S. H. Shenker, and D. Stanford(2015), arXiv:1503.01409